

High-Accuracy Indoor Localization Based on Chipless RFID Systems at THz Band

MOHAMMED EL-ABSI¹, ALI ALHAJ ABBAS¹, ASHRAF ABUELHAIJA², FENG ZHENG¹,
KLAUS SOLBACH¹, AND THOMAS KAISER¹, (Senior Member, IEEE)

¹Institute of Digital Signal Processing, University of Duisburg-Essen, 47057 Duisburg, Germany

²Electrical Engineering Department, Applied Science Private University, Amman 11931, Jordan

Corresponding author: Mohammed El-Absi (mohammed.el-absi@uni-due.de)

This work was supported by the German Research Foundation (DFG) for the CRC/TRR 196 MARIE, Project S04.

ABSTRACT Highly accurate indoor localization based on significantly low complex infrastructure has recently gained great interest for a variety of innovative location-based applications. In this regards, the chipless radio frequency identification (RFID) system is presented to be the low-cost solution, while time-based ranging using the ultrawide-band spectrum is promising to offer precise ranging capability. However, the current wide-band systems suffer from the spectrum and power limitations, which restrict the function of chipless RFID-based localization systems. Therefore, we propose terahertz (THz)-based chipless RFID localization system that enables a smart object localizing itself using the infrastructure composed from reference chipless tags. In more details, THz band offers huge bandwidth providing superior-resolution localization and large coding capacity. Moreover, we utilize the combination between dielectric resonator (DR) and lens to be designed as a frequency-coded chipless tag, where this combination increases the radar cross section of the chipless tags and, hence, extends their coverage zone. This cost-efficient design of the tag enables the dense deployment of low-cost infrastructure acting as reference anchors. Furthermore, we investigate the link budget of the proposed system in order to characterize the tag and distance-dependent spectral windows that are feasible for RFID-based localization. Afterward, the time-domain backscattered signal from a DR-Lens tag is analyzed in order to perform ranging and to calculate the relative distances between the DR-Lens tags and the reader leading to determining the reader position. Measurements are performed to prove the concept of the DR-Lens tag, while the numerical simulation is conducted to evaluate the proposed localization system. Simulation results show that the proposed system can reach superior accuracy of millimeter-levels.

INDEX TERMS Localization, RFID, large-scale MIMO, chipless RFID, dielectric resonator (DR), lens, RToF, estimation accuracy.

I. INTRODUCTION

Terahertz (THz) (0.1 – 10 THz) band communication is promising to play a vital role in the upcoming technology revolution, due to the vast range of opportunities and services that can be granted at this frequency band. The unprecedented large bandwidths offered at THz band, orders of magnitude greater than at the lower-frequency bands, is becoming a novel candidate not only for cellular systems but also for nano-networks, 3D imaging, spectroscopy, sensing, quality control. Specifically, this band provides localization, sensing and imaging applications the superior time-resolution leading to high accuracy performance [1]–[3].

Accurate indoor localization has recently gained great interest for a variety of future location-based services, such as internet of things (IoTs) and robotics [4]. Moreover, passive radio frequency identification (RFID) technology becomes a key-enabler candidate for indoor localization due to their energy harvesting capabilities and low complexity [5]–[8]. In particular, chipless RFID technology has more potential to be pervasive, since chipless tags contain neither battery nor chip, thus making them an extremely low-cost solution and applicable for the mass deployment for a wide range of applications [9]. Furthermore, chipless tags do not need energy harvesting thereby overcoming the disadvantage of passive tags that the intrinsic power consumption of

their chips is very challenging for operating at acceptable distances [10]. The main concept of chipless RFID technology is that the reader interrogates and communicates with the tags through the backscattered signal. Therefore, an RFID communication has two distinct links: the forward link for interrogating the tags, and the backscatter link for conveying the information from the tags to the reader [11].

Object localization requires the existence of two or more anchor nodes with known positions to determine the location of the object via noisy ranging techniques such as Time of Flight (ToF), Angle of Arrival (AoA), Received Signal Strength Indicator (RSSI), etc [12]–[15]. Among these ranging techniques, roundtrip ToF (RToF) based ranging technique is more conventional for passive and chipless RFID systems because of the backscattering communication, where RToF ranging utilizes the reader clock and thus does not require clock synchronization between the reader and the tag [16]. RToF accuracy is limited by multipath propagation, which affects the standard deviation of time measurement error. Accordingly, increasing the bandwidth leads to higher resolution of RToF estimation and more accurate localization. Therefore, the available bandwidth imposes a fundamental limit on the achievable accuracy for RToF based localization. Accordingly, recent studies have proposed to use the ultra-wide band (UWB) technology at the microwave band in order to utilize the available wideband spectrum to increase the accuracy of localization [17]. Unfortunately, due to UWB power regulations constraints and the batteryless chipless tags, it has been shown that chipless RFID based localization using UWB is strongly limited in communication range [18]–[20]. Moreover, UWB systems suffer from the dense multipath, especially in indoor environments, leading to a challenge in detecting the direct path signals [12]. Furthermore, the UWB spectrum limits the employment of massive chipless tags due to coding capacity [21].

In order to overcome the aforementioned limitations, we propose to fuse the advantages of THz band along with RToF based chipless RFID localization systems in order to achieve high-accuracy localization in indoor environments. Accordingly, we propose to use the combination between dielectric resonator (DR) and lens as a chipless tag, which meets the needs for simple design enabling the dense tag infrastructure. Additionally, the use of the THz frequency band is envisioned to offer huge bandwidth, which provides superior-resolution localization and large coding capacity opportunity. Moreover, the restrictions on power emission at THz band are expected to be less strict compared to the UWB band. Nevertheless, the huge bandwidth comes at the price of severe path loss due to the extra atmospheric attenuation in addition to serious reflection and scattering loss, which leads to a strict limitation on ranging distance [22], [23]. This limitation is fundamentally different and more severe in RFID systems compared to conventional communication systems because ranging in RFID systems involves two distinct links: the forward link and backscatter link.

Thanks to the very small wavelength at THz frequencies, we propose a novel chipless RFID localization systems with large-scale antennas at the reader side and DR-Lens combination at the tag side to combat the severe path loss aiming at reaping the distance limitation and improving localization accuracy. We study the link budget of the proposed system, and also we present the distance and tag dependent ranging limitations at THz band considering the RFID backscattered channel in order to characterize the tag and distance dependent spectral windows that are feasible for RFID based localization. Afterwards, we analyze the time-domain backscattered signal from a DR-Lens tag in order to extract the RToF between this tag and the reader from the backscattered signal at the reader. Accordingly, the relative distances between the DR-Lens tags and the reader are calculated, eventually then the reader position is determined using linear least square (LLS) approximation. Due to ongoing research on DR tag miniaturization towards sub-mm dimensions for achieving THz-functionality, first measurements are performed in the GHz-range to prove the principal functionality of the DR-Lens tag, while numerical simulations are carried out in the THz-range to evaluate the overall localization system considering various topologies of the infrastructure. These results show that the proposed method can achieve superior accuracy of millimeter-levels.

This paper is organized as follows: we give a discussion of related work in Section II. The system model is described in Section III. We present in Section IV the DR-Lens tag based ranging at THz Band. Section V presents the proposed chipless RFID based localization at THz band. Measurements and simulative results are reported in Section VI. We conclude our work in Section VII.

II. RELATED WORK

Recently, passive RFID based localization received much interest not only in today's applications but also for the ongoing research in order to provide high accuracy localization with low complexity. The major focus in literature is the merge between RFID and ultra-wide band (UWB) technologies to utilize the large bandwidth provided by UWB technology to increase the ranging accuracy [24]. Ranging methods are severely influenced by the wideband statistics of the backscatter channel. The achievable ranging performance is analyzed for UWB systems, where the Cramér-Rao lower bound (CRLB) and the Ziv-Zakai bound are derived [24]–[26]. The bandwidth scaling is analyzed for RFID positioning in dense multipath scenarios in [27], where the ranging error variance for correlated and uncorrelated backscatter channels is developed. In [12], wide-band RFID is evaluated using measurements, where the Rician K-factor for the line-of-sight (LoS) component, the root-mean-square (RMS) delay spread, and the spaced distance correlation function are analyzed. Additionally, Decarli *et al.* [28] study the architecture and protocol of UWB RFID systems considering the practical issues of localization systems.

Recently, few studies investigate the characterization of backscatter signals at mm-wave [29]–[31]. Moreover, the work in [32] investigates the possibility of passive RFID localization based on millimeter-wave backscattered signals with a single reader equipped with high directivity beam-steering antennas. El-Sayed *et al.* [34] study the performance of localization algorithms at the millimeter band in terms of both mean square estimation error and average error. Wang *et al.* [32] investigate the feasibility of ranging and positioning in millimeter level accuracy using millimeter-wave and three-dimensional massive antenna arrays using lower bounds derivations.

Other efforts concentrating on chipless RFID localization are performed as in [34]–[36]. 3D space localization using printed chipless RFID is presented in [34] by using a frequency domain chipless tag, where the chipless tag is interrogated by an ultra-wideband signal. Zhou *et al.* [35] propose short-range wireless localization based on meta-aperture and compressed sensing by utilizing the nonlinear, multimodal plasmonic dispersion of a magnetically uniaxial metamaterial. In [36], a preliminary work is presented to use DR tag based localization in indoor environments, where the ringing behavior of the DR tags is utilized as the fingerprint of the tags.

III. SYSTEM MODEL

In this work, we propose a chipless RFID based localization system operated at THz band. We consider device based localization also called self-localization, where an object not aware of its position is usually equipped with an RFID reader to collect information and realize the environment using the reference nodes, i.e. chipless tags responses, as well as the stored infrastructure information to obtain its relative location.

Since THz band offers wide bandwidth spectral windows, RTof based localization is preferable to be used due to the expected superior time-resolution even in dense multipath environments [27]. Moreover, there is no clock drift at the tag side which could affect the RTof localization of the backscattered pulse since RTof is determined only by the reader, which is equipped with a high-accuracy clock [16].

An object can obtain its relative position through two steps: ranging and lateration. The first is performed in a way that the reader measures the RTof from all the available tags and estimates the distances between the reader and the tags. The latter is executed to find the position of the reader using the distances obtained from the first step by means of the trilateration algorithm, which is a geometrical method that can localize the object based on its Euclidean distance from three or more tags [37].

Next, more details about the system design are presented.

A. SYSTEM CONFIGURATION

Specifically, we consider a 3D indoor environment area with dimension $w_1 \times w_2 \times w_3$, in which an RFID localization network is assumed with N chipless tags, i.e. the reference

nodes. Let $\mathbf{p}_n = [x_n, y_n, z_n, f_n]^T \in \mathbb{R}^4$, $n \in \{1, 2, \dots, N\}$ be the known settings of the n^{th} tag, where x_n , y_n and z_n are x-, y- and z- coordinates of the tag, respectively; and f_n is the resonance frequency of the tag. The reference nodes are nested at the ceiling of the indoor environment as shown in Fig. 1.

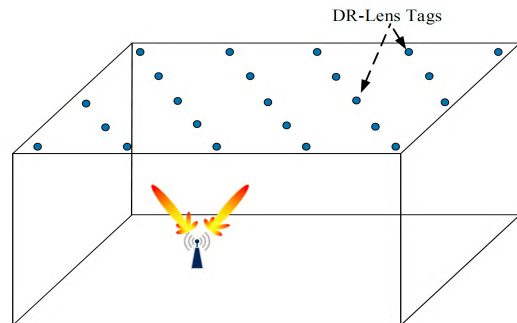


FIGURE 1. RFID localization system.

The reader has fixed antenna aperture of A_R in order to obtain G_R as the gain of the reader. Denote $\mathbf{p}_r = [\bar{x}, \bar{y}, \bar{z}]^T \in \mathbb{R}^3$ to be the reader coordinate vector to be estimated.

B. TAG SETUP

In this work, we consider passive and chipless tags to act as anchors for the localization system. The major advantage of these tags is their passivity, which means that the energy consumption is low since the energy of the tag is drawn from the reader without a need for external power source (or battery) to operate, and in addition the tag is chipless. The DR as a chipless tag has inspired recent applications such as sensor systems [38], [39]. However, DR chipless tags suffer from low radar cross section (RCS) especially at THz bands, which makes the detection of such tags difficult even impossible.

Recently, we have proposed a combination between the DR and a dielectric spherical lens in order to enhance the RCS of the chipless tag [40]. In this combination, the spherical lens collects the interrogator incident wave power across the lens aperture and concentrates it to a focal area behind the lens surface, where a DR is placed at this point acting as a receiving antenna. Then, the resonant modes of the DR are excited at a level proportional to lens antenna gain, and the DR retransmits the incident power through the mode radiation patterns which couples part of the power back into the lens, providing gain as in a transmit lens antenna.

A DR, which is the first part of the combination, reflects the reader signal in the direction of the incident wave with increased RCS at specific resonance frequencies depending on DR size, dielectric constant and excited mode. In order to obtain the behaviour of DR tag close to realistic conditions, the DR tag is constructed in CST Microwave Studio as a three-dimensional (3D) model, and full-wave electromagnetic simulation is performed. The RCS of a single ceramic

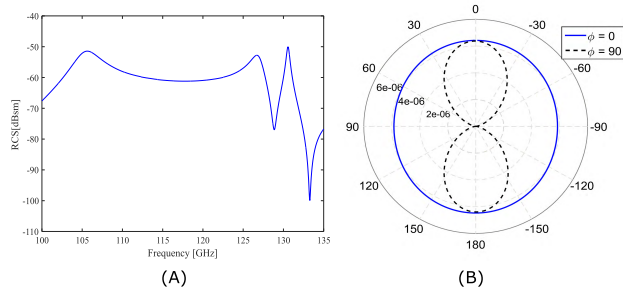


FIGURE 2. A: Monostatic RCS of a single DR Tag. B: Single DR bi-static scattering at 105.6 GHz resonance frequency on plane $\phi = 0$ and $\pi/2$ for wave incident along z-axis.

cylindrical resonator with relative permittivity of 35, that has a radius of 0.310 mm and height of 0.291 mm, is simulated, where Fig. 2.A shows the RCS spectrum with RCS values -51.94 , -53.68 and -49.39 dBm² at resonance peaks around 105.6, 126.1 and 130.4 GHz respectively. It is seen that the RCS values at THz frequencies are relatively small, which makes the detection of DR tags a challenging problem. Fig. 2.B shows the bi-static RCS pattern at the first resonance frequency $f = 105.6$ GHz. When a DR tag is excited at 105.6 GHz, the DR radiates as a magnetic dipole [41] oriented perpendicular to the DR axis as seen in Fig 2.B.

A spherical homogeneous lens, which is the second part of the combination, is used to enhance the low scattering response of the DR, where the DR is positioned behind the surface of the lens creating high gain beams with gain approximately proportional to the lens aperture. Homogeneous dielectric spheres are easy to fabricate by molding or machining from low-loss plastic material, like Polypropylen, Polyethylene, etc, and are readily available from industrial manufacturing for ball bearings. In the simulation, it is assumed that the homogeneous material has a rel. permittivity of $\epsilon_r = 2.22$.

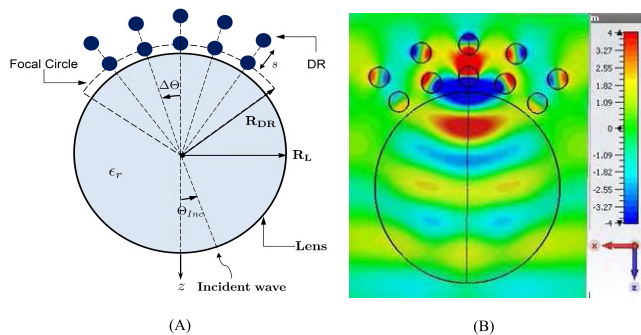


FIGURE 3. A: DR-Lens combination for wide angle of incidence B: Field distribution (E_y -field) in the central cross-sectional plane of the Lens-DR tag with $\Delta\Theta = 20^\circ$ and $\Theta_{Inc} = 0^\circ$.

Fig. 3.A presents the proposed DR-lens combination that will act as a reference tag in the proposed localization system [40]. Five pairs of DRs are located along the focal line at radius $R_{DR} = 3.398$ mm behind the lens of radius

$R_L = 2.9125$ mm at an angular shift $\Delta\Theta = 20^\circ$, where the distance between DR in each pair is $s = 0.9708$ mm. A pair instead of single DR at each focal position improves signal contrast at the lowest (fundamental) resonant mode frequency, which attains the spectral fingerprint after amplification through the gain of the lens [40].

When we excite the DR-lens combination by a plane wave with $\Theta_{Inc} = 0^\circ$, the middle DR pair is excited, and a retro-directive scattering with maximum monostatic RCS level is generated. Fig. 3.B shows the field distribution in the central cross-sectional plane of the Lens-DR tag for $\Theta_{Inc} = 0^\circ$ at 105.6 GHz frequency. It is observed that the fields are collimated towards the other side of the lens in a “quasi-focal region” exciting the middle DR pair with maximum amplitude while the adjacent pairs are excited with lower amplitude.

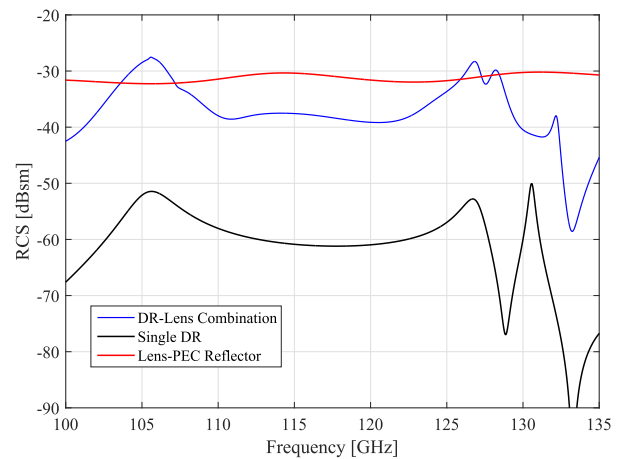


FIGURE 4. Monostatic RCS of DR array for DR-Lens configuration compared to DR pair configuration.

Fig. 4 shows the improvement in mono-static RCS of DR-Lens combination compared to single DR, where the RCS of DR-Lens tag is -27.52 dBsm at 105.6 GHz compared to -51.94 dBsm for single DR at the same resonance frequency. Furthermore, the DR-Lens tag shows higher RCS at the resonance modes compared to lens perfect conductor (PEC) reflector combination by approximately 4 dB, which emphasizes the high efficiency of DR as a reflector in combination with lens. By the same mechanism, the other pairs are excited when Θ_{Inc} varies aiming at covering a wider angle of incident waves with high RCS. It is noteworthy here that $\Delta\Theta = 20^\circ$ is chosen to maintain the maximum acceptable variation of the created retro-directive RCS as a function of the angle of incidence Θ_{Inc} [40]. Fig. 5 depicts the variation of RCS when the angle of incidence Θ_{Inc} varies between -45° to 45° , where the change is limited up to ± 2 dB for $\Delta\Theta = 20^\circ$. The design in Fig. 3.A provides us with retrodirectivity property in one plane within the range of -45° to 45° , where the arc linear array could be complemented by vertically staggered arrays in order to generate two-plane retrodirectivity.

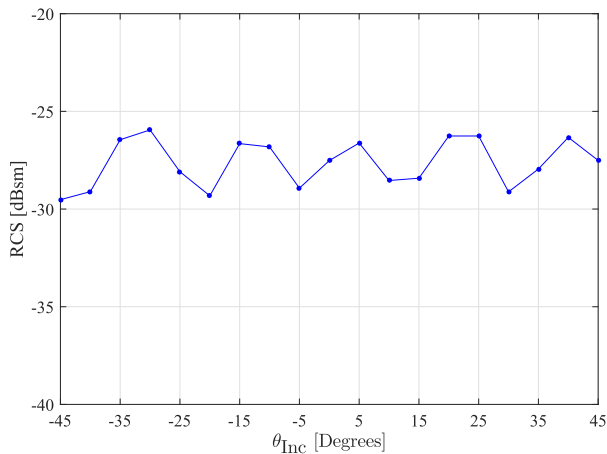


FIGURE 5. RCS variations with the angle of incidence.

Last but not least, huge bandwidth available at the THz band offers a potential opportunity to maximize the coding capacity using frequency coding leading to the possibility of manufacturing many chipless DR tags as in [21] and [43] and references therein. The detailed design of frequency-coded DR tags is out of this paper scope.

C. MODELLING OF RFID BACKSCATTER CHANNEL AT THz BAND

We inspect the RFID backscatter channel consisting of a forward channel from the RFID reader to a DR-Lens tag and a backward channel from the tag to the RFID reader. The propagation mechanisms and environment interaction influencing a wireless transmission at the THz band are dissimilar to the communications at the lower frequency bands. THz communications suffer from the severe absorption properties of atmospheric gases leading to a very high and frequency-selective path loss for LOS links [22], [23]. Furthermore, the THz channel is governed by a high reflection loss, where only up to second order reflections are noticeable and have to be considered in the THz communication modeling [22].

Due to the mentioned specific nature of THz band, the operation of RFID systems at THz band should be investigated in order to analyze its practical feasibility and overcome the channel and hardware limitations. Particularly, the analysis of the RFID link budget at the THz band should take into account the mentioned limitations aiming at achieving robust and successful RFID communications by assuring that the received scattered power at the reader at the backward channel is higher than the sensitivity of the reader.

As the chipless DR-Lens tag can be modelled to be an antenna with a short circuit termination, the power impinging on the n^{th} DR-Lens tag at the forward link at frequency f_o is [43]

$$P_{t,n}^{f_o} = \rho_n P_T G_R G_T^{f_o} L(d_n, f_o), \quad (1)$$

where ρ_n presents the polarization loss factor due to the mismatch between the polarization of a reader antenna and the n^{th} DR-Lens tag. The power transmitted from the RFID reader is P_T , where the antenna gain of the reader is G_R and identical at all frequencies.

The gain of the n^{th} DR-Lens tag at frequency f_o is denoted by $G_T^{f_o}$ and expressed as

$$G_T^{f_o} = \frac{\sqrt{4\pi\sigma_n^{f_o}}}{\lambda_o}, \quad (2)$$

which is a function of the tag RCS $\sigma_n^{f_o}$ at frequency f_o , and the wavelength of the carrier frequency λ_o .

The term $L(f_o, d_n)$ is the resulting channel pathloss between the reader and the n^{th} tag at the carrier frequency f_o when the distance between them is d_n . The channel impulse response between the reader and the n^{th} tag is denoted by $h_n(t, d_n)$, where this channel is modelled at THz band using the modified Saleh-Valenzuela (S-V) model as [22], [23]

$$h_n(t) = \alpha_{\text{LOS}}^n(f_o, d_n) \delta(t - \tau_{\text{LOS}}^n) + \sum_{r=1}^{R_n} \alpha_r^n(f_o, d_r) \delta(t - \tau_r^n), \quad (3)$$

where α_{LOS}^n and τ_{LOS}^n refer to the attenuation and time delay of the LoS path between the source and the n^{th} tag. Assuming R_n reflected rays, α_r^n and τ_r^n are the attenuation and time delay of the r^{th} reflected path, which has length d_r . Accordingly, $L(f_o, d_n) = |H_n(f, d_n)|^2$, where $H_n(f, d_n)$ is the frequency domain channel response.

At THz band, the LoS attenuation α_{LOS}^n consists of the spreading loss and the molecular absorption loss, which is expressed as

$$|\alpha_{\text{LOS}}^n(f_o, d_n)|^2 = L_S(f_o, d_n) L_A(f_o, d_n), \quad (4)$$

where the spreading loss L_S is defined as

$$L_S(f_o, d_n) = \left(\frac{\lambda_o}{4\pi d_n} \right)^2, \quad (5)$$

while the molecular absorption loss L_A is defined as

$$L_A(f, d_n) = e^{-k_A(f_o) d_n}, \quad (6)$$

where k_A is the frequency-dependent medium absorption coefficient. Accordingly, the attenuation of the reflected paths α_r^n is defined as

$$|\alpha_r^n(f_o, d_r)|^2 = \bar{\Gamma}_i(f_o) L_S(f_o, d_r) L_A(f_o, d_r), \quad (7)$$

where $\bar{\Gamma}_i(f_o)$ is reflection coefficient of the i^{th} reflected path.

The total received power backscattered from the n^{th} tag at the reader is [43]

$$\begin{aligned} \bar{P}_n^{f_o} &= \rho_n^2 P_T |G_T^{f_o} G_R L(d_n, f_o)|^2 \\ &= \frac{4\pi}{\lambda_o^2} \sigma_n^{f_o} \rho_n^2 P_T |G_R L(f_o, d_n)|^2. \end{aligned} \quad (8)$$

In (8), the monostatic RFID is assumed, where the extension to bistatic case is straightforward.

IV. DR-LENS TAG BASED RANGING AT THz BAND

The RToF ranging technique, which is also known as two-way ranging, is used in the proposed system due to its superior time-resolution and the simple required clock synchronization. RToF determines the distance between the reader and a reference DR-Lens tag by measuring the complete round-trip TOF of signal between the transmitter and the receiver.

This section illustrates the influence of THz band on RToF ranging considering the practical limitations of this band. Moreover, we present how to extract the RToF information from the backscattered signal from the DR-Lens tag.

A. RANGING COVERAGE AT THz BAND

In this part, we will consider the ranging coverage of the RFID localization network at THz band considering the practical limitations such as THz channel and DR-Lens tag hardware limitations.

Since the DR-Lens is a chipless tag, its backscatter signal power at the reader is proportional to the tag RCS and has no sensitivity limit. From another point of view, an RFID reader must be able to detect the backscattered signals from the tag, which relies on the reader antenna sensitivity. Accordingly, the received power $\bar{P}_n^{f_o}$ must be above the reader limit of detection power in order to be detected.

The RFID link path loss is many orders of magnitude weaker than one-way link communications, since the RFID communication requires two cascaded links in addition to the practical limitations of the tags such as its low RCS. This situation is more severe at THz band compared to the lower bands, due to the extreme attenuation loss and the transmission windows created by molecular absorption leading to a very high and frequency-selective path loss for LOS links [22], [23]. Accordingly, the communication distance plays a vital role in specifying the bandwidth of the transmission windows.

The spectral windows, in which an RFID communication link can be initiated, are characterized using the path loss threshold L_{th} considering the distance and the structure of the tag in order to guarantee the minimum single-pulse signal-to-noise ratio (SNR) threshold β of the desired backscattered signal at the receiver, where this threshold β guarantees the probability of detection to be not less than 99%. Accordingly, the spectral windows are specified to have path loss smaller than the threshold L_{th} , that is expressed as

$$2L_{th}[\text{dB}] = P_T[\text{dBW}] + 2G_R[\text{dBi}] + 2G_T^{f_o}[\text{dBi}] + G_P + 10 \log \left(\rho_n^2 \right) - P_w[\text{dBW}] - \gamma - \beta, \quad (9)$$

where G_P is the processing gain that can be achieved using signal processing techniques. γ is the factor that takes into account the noise figure and other channel and hardware impairments. P_w is the noise power, which has two major sources. The first is the frequency-dependent and colored noise in the THz band channel, which is caused by the molecular absorption noise. The second major noise source is the thermal noise which comes from the electronic circuits of the

devices. The noise power can be evaluated using

$$P_w = kB(T_{mol}(f_o, d) + T_{other}(f_o)), \quad (10)$$

where k is Boltzmann constant, $T_{mol}(f_o, d)$ is the molecular noise temperature, $T_{other}(f_o)$ is the temperature of other sources of noise at the frequency f_o , and B is the bandwidth [44], [45]. The molecular noise is only considerable around the frequencies in which the molecular absorption is considerably high [45].

Considering the hardware capabilities at THz band in the literature, the reader transmit power can be considered to be $P_T = 0$ dBm. Moreover, the processing gain of $G_P = 40$ dB can be practically achieved using coherent and non-coherent integration, especially in localization systems due to the possibility of many times of pulse repetitions [46]. More processing gain is limited due to short-time stability characteristics of the reader such as jitter, phase and quantization noise [47]. Tag detection at the reader can be performed using many algorithms as in [48]–[50] and references therein achieving more than 99% detection probability when $\beta = 20$ dB. Up to 500 GHz, the noise figure γ can be approximated to be 20 dB [44]. We assume that the reader has an area for the antenna of $A_R = 100$ cm² with ideal aperture efficiency. According to the design of the tag in Section III-B, the effective area of the DR-Lens combination at 100 GHz equals $A_T = 33.7$ mm².

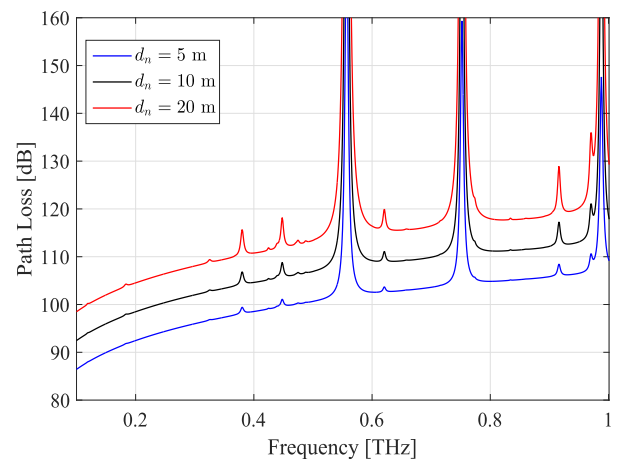


FIGURE 6. Free space path loss for LoS path at THz band for different distances.

Recalling (5), the free space path loss grows with the square of the frequency λ_o^{-2} as shown in Fig. 6, where this figure shows the path loss for LoS path at THz band for different distances using the relation in (4). This can be overcome by using fixed-area antennas, which enables the increase of antenna gain proportional to λ_o^{-2} . In addition to the hardware capabilities at THz band and path loss, the coverage of an RFID system at THz is influenced by the aperture area of the antennas at the reader and the tag sides. This influence can be summarized in three cases:

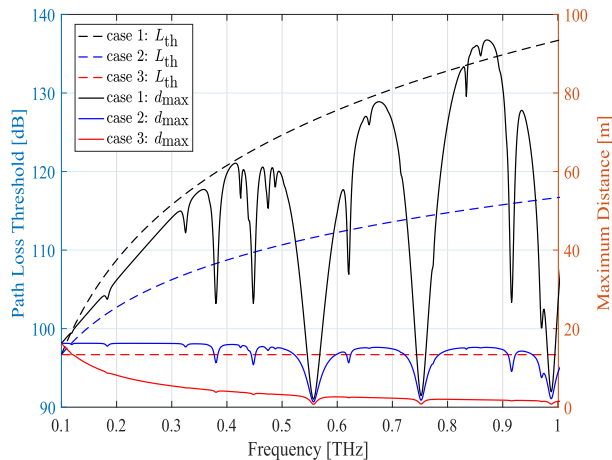


FIGURE 7. Path loss threshold and the maximum LoS distance versus the frequency for the three design cases.

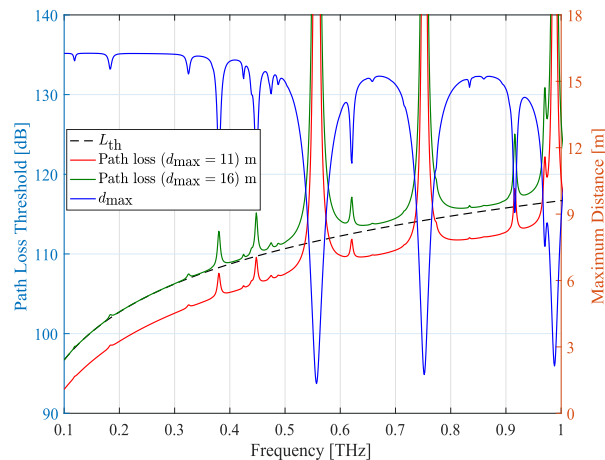


FIGURE 8. Path loss threshold and the maximum LoS distance versus the frequency for the DR-Lens tag based RFID system.

- *Case 1:* When the reader and the tag have fixed-area antennas, i.e. A_R and A_T respectively, the antenna gain of the reader and the tag increase proportional to λ_o^{-2} . Accordingly, the path loss threshold increases proportional to λ_o^{-4} , which yields more spectral windows for communications and better coverage for the RFID system at THz band as seen from Fig. 7 for $A_R = 100 \text{ cm}^2$ and $A_T = 33.7 \text{ mm}^2$. Moreover, this increase not only overcomes the path loss absorption, but also improves the system coverage as depicted from Fig. 7, where this figure shows the maximum LoS distance d_{max} that can be covered by the RFID system versus the frequency. The degradation of d_{max} especially above 350 GHz is a result of the path loss peaks caused by the molecular absorption. These absorption peaks create spectral windows, which have different BW, and drastically change with the variation of the frequency.
- *Case 2:* When the tag antenna has constant gain and the reader has fixed-area antennas, the antenna gain of the reader increases proportional to λ_o^{-2} . Accordingly, the path loss threshold increases proportional to λ_o^{-2} as seen from Fig. 7 for $G_T = 16.7 \text{ dBi}$ and $A_R = 100 \text{ cm}^2$, which is the same increase rate as that of the path loss absorption. Thus, the reader antenna gain compensates the path loss with the change of the frequency leading to constant coverage for the RFID system at THz band as shown from Fig. 7. The degradation of coverage at some frequency bands is a result of the path loss peaks caused by the molecular absorption.
- *Case 3:* When the reader and the tag have fixed antenna gains, the path loss threshold is constant, and, hence, the coverage of the RFID system at THz band is decreased by the frequency increase as shown from Fig. 7 for $G_R = 40 \text{ dBi}$ and $G_T = 16.7 \text{ dBi}$.

In our system model, the tag is designed as a DR-Lens combination, where the geometrical dimensions of the tag play a vital role in identifying mode frequencies of the tag.

Therefore, the gain of the tag is kept constant and, hence, case 2 is consistent with the considered system model. According to the design of the tag in Section III-B, the antenna gain of the tag equals $G_T = 16.7 \text{ dBi}$. Fig. 8 shows the path loss threshold of the considered system model in addition to the maximum LoS distance d_{max} that can be covered by the RFID system versus the frequency. It is noted that the path loss peaks create spectral windows with different bandwidth. According to Fig. 8, the maximum ranging distance that can be covered is approximately 16 m in order to guarantee $\beta = 20 \text{ dB}$. Fig. 8 shows also the free space path loss for $d_{\text{max}} = 16 \text{ m}$, where the spectral windows can be identified when the free-space loss is smaller than the path loss threshold. Consequentially, the spectral windows for ranging with the maximum distance can be performed in the following spectral windows with total bandwidth of 0.23 THz: 0.1-0.184 THz, 0.194-0.318 THz, and 0.336-0.358 THz. In order to obtain wider spectral windows and consider low-level molecular absorption, the maximum ranging can be limited to approximately 11 m. Fig. 8 shows also the free space path loss for $d_{\text{max}} = 11 \text{ m}$, where the spectral windows can be identified for ranging with coverage less than 11 m in the following spectral windows of total bandwidth of 0.724 THz: 0.1-0.534 THz, 0.582-0.733 THz and THz.

From a practical point of view, the spectral window 0.1-0.534 THz is more suitable, since the required reader antenna gain can be attained, and also the noise figure is guaranteed to be less than 20 dB. Therefore, the system can be designed to operate within this spectral window depending on the hardware limitations.

B. RToF ESTIMATION FROM THE BACKSCATTERING SIGNAL

In this part, we present the backscattered signal from the chipless DR-Lens tag designed in Section III-B in order to extract RToF between the reader and a reference tag. The transmitted

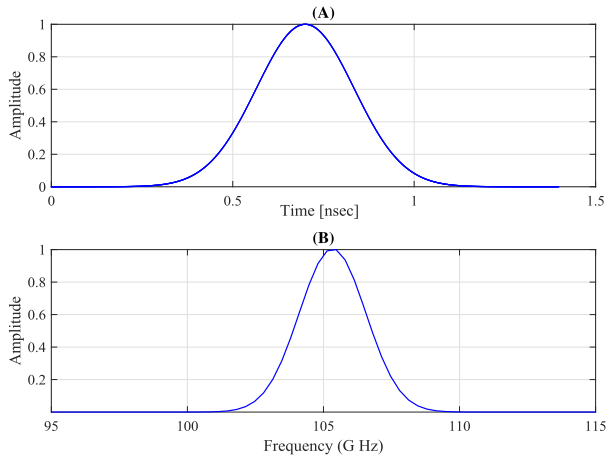


FIGURE 9. A: Envelope of a Gaussian RF pulses with 5GHz bandwidth. B: Frequency spectrum of the pulses.

interrogation pulse can be expressed as

$$x(t) = A_o \cos(2\pi f_c t) \exp\left(-\frac{(t - \nu)^2}{2\sigma_x^2}\right), \quad (11)$$

where A_o and f_c are the amplitude and the carrier frequency of the pulse, respectively. ν and σ_x are the parameters that define the shape and the bandwidth of the Gaussian pulse. The interrogation pulse is designed according to the predefined frequency-code of the chipless RFID tag that is considered in Section III-B. Fig. 9 shows the envelope and the spectrum of a Gaussian pulse with bandwidth 5 GHz covering a 3-dB bandwidth of the resonance frequency of the DR-Lens tag at 105.6 GHz.

When a DR-Lens tag is interrogated with a pulse signal, the backscattered signal from the tag has two scattering modes [51], which are: 1) structural mode and 2) resonator mode. The structural mode is caused by the reflecting part of the incident wave caused by the size and shape of the structure of the DR-Lens tag. The resonator mode results from the interaction between the DR and the incident wave.

The principal behavior of the electromagnetic (EM) scattering response of the DR tag is investigated and studied by measurements and simulations in [52]. It is found that the structural reflection from the considered DR tag superimposes the resonator mode, which is due to the multi-pole displacement current source excited inside the dielectric material; its level is found about 15 dB below the fully excited resonator mode response.

The pulse duration, which is inversely proportional to the bandwidth B , plays a vital role in DR behavior, where it affects the delay and pulse amplitude of the DR pulse response. In order to obtain the maximum DR pulse scatter amplitude (the effective RCS) and a known fixed delay response due to the charging process, the DR has to be fully charged up [52]. Consider the DR resonant mode at 105.6 GHz with a 3-dB bandwidth of 3.86 GHz, which leads to a quality factor (Q-factor) of 27.35 and the time

constant (τ_{DR}) of 82.46 psec. We assume that the pulse duration should be at least $8\tau_{DR}$ in order to guarantee the full charge of the DR-Lens tag, which, however, limits the time resolution.

Using the Gaussian excitation radio frequency (RF) pulse presented in Fig. 9, where its peak is centered at 0.71 n sec, the normalized time-domain reflected signals for two cases are shown in Fig. 10.A and Fig. 10.B using EM simulation when the tag is placed 50 cm and 100 cm away from the reader antenna, respectively. The position of the tag is assumed to be the center of the lens. The first case titled “Resonant” shows scattering from a DR-Lens tag resonant mode at 105.6 GHz, while the second titled “Non-Resonant” shows scattering from a DR-Lens tag with smaller DR with resonant mode at 113 GHz.

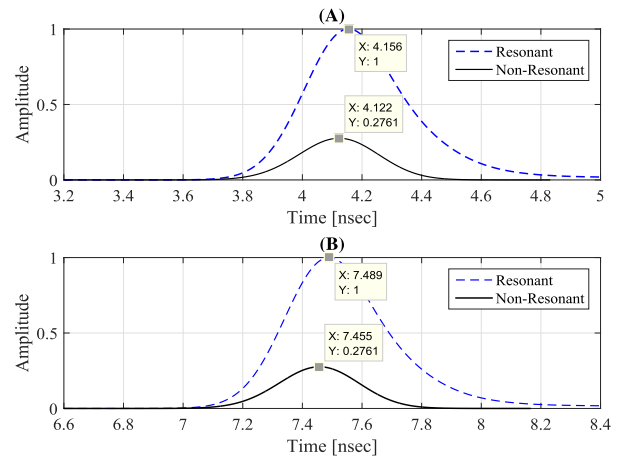


FIGURE 10. Normalized time-domain reflected signals at resonant and non-resonant for different distances between the reader and the DR-Lens tag. A: 50 cm B: 100 cm.

We see from Fig. 10 that when the frequency of the incident signal does not match the resonant frequency, the tag response is much smaller than in the resonance case; 11 dB lower in the simulated scenario as shown in Fig. 10. Therefore, the multi-tag interference is highly reduced and, hence, the desired received backscattered signal quality is improved.

From another side, the peaks of the reflected signals should be centered at 4.043 nsec and 7.376 nsec for 50 cm and 100 cm distances in case of free space propagation, respectively. However, it is noted from Fig. 10 that the peaks of the reflected signals at resonance and non-resonance cases are delayed and allocated respectively at 4.156 and 4.122 nsec at 50 cm distance and 7.489 nsec and 7.455 nsec at 100 cm distance. Generally, the delay results from: 1) DR charging-up, and 2) the wave travelling through the dielectric material of the lens. Additionally, the interaction between the excitation signal and the structure of the tag results in an additional delay since the exact source point (also known as “phase centre” in antenna theory) of the reflection from a tag is unknown. When the tag at resonance case, it is affected by the reasons of the delay leading to a delay of 113 psec as noted from

Fig. 10 for 50 cm and 100 cm distances. Therefore, this delay could be estimated for each resonance frequency in order to be considered and calibrated when estimating the RTof. Considering the non-resonance case, the delay is estimated to be 79 psec, which is a result of the wave travelling through the dielectric material of the lens. If the pulse duration does not fully charge the tag, the delay will be less than in the case of fully charging the DR-Lens tag [52].

Hardly visible, the tail of the resonant mode response has a lower decay rate than the tail of the metal scatter, which is due to the discharging of the resonator (also called “ringing”).

V. RFID BASED LOCALIZATION AT THz BAND

For unambiguous localization in a 3-D plane, a minimum of four anchors, i.e. chipless DR-Lens tags in our case, are required [53]. The DR-Lens tags are nested at the ceiling of the environment as shown in Fig. 1, where the minimum separation between the adjacent tags is Δ . Due to the extremely low complexity and price of the designed DR-Lens tag, we propose the dense deployment of the DR-Lens reference tags in order to achieve three goals. The first goal is to guarantee that at least four tags are in the range of the reader due to the distance limitation at THz band. The second goal is to enable the high directional reader to perform ranging for closer tags with minimum scanning efforts and high SNR. The third goal is to offer the possibility for ranging more than four reference tags aiming at increasing the localization accuracy.

The localization algorithm is performed through three phases: The first is scanning phase; the second is ranging phase; and the third is lateration phase.

A. SCANNING PHASE

At the first phase called scanning phase, the reader performs a fast and rough scanning with an angular separation ϕ_s . The reader is able to beamform the transmitted signal using the steering vector toward a specific direction [54], whereas the tags respond by backscattering the received signal back to the reader position using the retrodirectivity property of the tag. Accordingly, for a given direction, the reader sweeps the whole frequency band in which the tags are coded, i.e. within the band 0.1-0.534 THz, in order to detect the reference tags that are allocated at the predefined direction. This process can be performed using a pulse that covers the whole bandwidth or using a frequency modulation signal that sweeps the whole frequency band during the t -second pulse duration with either fixed or adaptive hopping. The process of frequency sweeping mainly depends on the frequency-coding of the reference tags and, particularly, the position and the bandwidth of the anchors' resonance frequencies. After analyzing the backscattered signal, the different reference tags that fall into the same angle section are assigned into one tag group. Tags in different groups are spatially separated and, hence, do not interfere with each other. Thus, the distribution of tags should consider that the adjacent tags should have far resonance modes in order to reduce multi-tag interference.

The scanning algorithm is repeated until detecting at least four groups or more. Assume the reader has decided to have N_{Ref} reference tags to perform localization, where $N_{\text{Ref}} \geq 4$. Accordingly, the scanning phase continues until the reader finds N_{Ref} groups, where the g^{th} group is denoted by ψ_g .

B. RANGING PHASE

After tag grouping at the first phase, the ranging phase is executed in which the reader carries out ranging to only one tag within each group, i.e. the n^{th} tag within the g^{th} group termed as the T_n^g tag. This tag is chosen to have the lowest resonance frequency in order to minimize inter-tag interference with the other tags within the group. Accordingly, the reader transmits a signal that is centered at the resonance frequency of the T_n^g tag and covers the resonance bandwidth. Then the backscattered signal from this tag is post-processed using matched filter or maximum likelihood estimator in order to estimate RTof and then the distance between the reader the T_n^g tag as discussed in Section IV-B. The reader is expected to receive two types of backscattering signals. The first is the backscattered signal from the desired tag, which presents the resonance behavior at the resonant frequency of the DR-Lens tag as discussed in Section III-B. The second type is the inter-tag interference resulting from the backscattered signals from the other DR-Lens tags, where these signals are highly attenuated and degraded as mentioned in Section III-B. When ranging the T_n^g tag, the inter-tag interference is caused from the undesired tags that are located within the same group, i.e. the g^{th} group. These interfering tags are located within a disk area with radius R_g , i.e. the interference area around the desired tag, where this disk area is proportional to the reader's antenna beamwidth and the distance between the reader and the reference DR-Lens tags.

The interference from the T_j^g DR-Lens tag when the reader performing ranging with the T_n^g tag at its resonance frequency f_n is obtained by

$$I_j^{f_n} = \frac{4\pi}{\lambda_n^2} \sigma_j^{f_n} \rho_n^2 P_T |G_{RL}(f_n, d_j)|^2, \quad (12)$$

where $\sigma_j^{f_n}$ is the RCS of the j^{th} tag when it operates at frequency f_n . According to the design of DR-Lens tags, since the j^{th} tag has a resonance frequency f_j , $\sigma_j^{f_n}$ is much less than $\sigma_j^{f_j}$ and also $\sigma_n^{f_n}$.

Consequently, the instantaneous frequency-dependent SINR at the reader during the ranging of the n^{th} tag is defined as:

$$\xi_n = \frac{\bar{P}_n^{f_n}}{N_o + \sum_{j \in \psi_g, j \neq n} I_j^{f_n}}. \quad (13)$$

The antenna radiation pattern of the reader can be modelled as a single cone-shaped beam whose width determines the antenna directivity, where the side lobes are neglected due to their very low gain. Hence, the antenna gain G_R for the main

lobe in the cone model is presented as [55]

$$G_R = \frac{2}{1 - \cos(\varphi/2)}, \quad (14)$$

where φ is the antenna directivity angle as shown in Fig. 11 and $\varphi < 180^\circ$. For simplicity and without loss of generality, the coverage area of the reader antenna can be approximated as right circular cone. Accordingly, using the model in (14), the distance between the DR-Lens reference tags can be fixed in order to avoid inter-tag interference as

$$\Delta_m \geq d_{\max} \tan(\varphi/2). \quad (15)$$

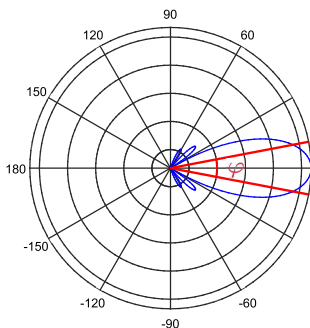


FIGURE 11. The model of a single cone-shaped radiation pattern.

Consequently, the presence of interference is dependent on the density of the anchors in the environment and the distance between the reader and the anchors.

C. LATERATION PHASE

After performing the ranging for one tag per each group, the position of the reader can be estimated using the estimated distances by means of the trilateration algorithm, which is a geometrical method that can localize the object based on its Euclidean distance from four or more tags. Algorithms as linear least square (LLS), weighted LLS (WLLS), singular value decomposition (SVD), or nonlinear least squares (Newton) method can be used to estimate the position of the reader from the estimated distances from ranging step [37]. The localization algorithm is summarized in Algorithm 1.

VI. MEASUREMENTS AND NUMERICAL SIMULATIONS

This section presents first measurements in the lower GHz-range to prove the principal functionality of the DR-Lens tag. Furthermore, numerical simulations are performed to evaluate the proposed chipless RFID based localization at THz band.

A. MEASUREMENTS

In this part, we present the first experimental verification for the DR-Lens combination designed at 10.1 GHz. Due to the unavailability of DRs manufactured at THz frequencies and depending on the concept of scale model measurements, the measurements are performed at relatively low microwave frequency range as a proof of concept. Five pairs of DRs

Algorithm 1 The Proposed Localization Algorithm

- 1: Determine the number of the required reference tags N_{Ref} .
- 2: The reader performs scanning phase to obtain N_{Ref} groups, i.e. $\{\psi_g\}$, $g = 1, 2, \dots, N_{\text{Ref}}$.
- 3: **for** $g = 1$ to N_{Ref} **do**
- 4: Select one reference tag within the group $\{\psi_g\}$ termed as the T_n^g tag.
- 5: The reader transmits the interrogation pulse that covers the resonance frequency of the T_n^g tag.
- 6: The reader estimates the RToF and then the distance between the reader and the T_n^g tag, i.e. \hat{d}_g^n .
- 7: **end for**
- 8: The reader estimates its position using trilateration algorithm.

are located along the focal line at radius $R_{\text{DR}} = 40$ mm behind the lens of radius $R_L = 30$ mm at an angular shift $\Delta\Theta = 20^\circ$, where the distance between DR in each pair is $s = 10$ mm. The DRs were manufactured by T-Ceram s.r.o. of Czech Republic and each DR has a radius of 3.2 mm and height of 3 mm with relative permittivity of 37.

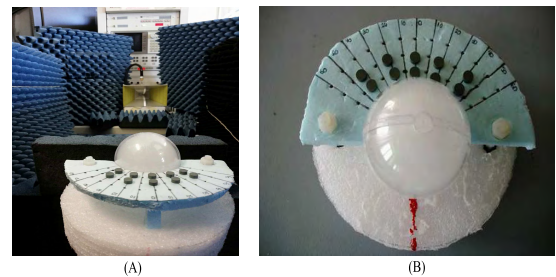


FIGURE 12. The measurement setup. A: Double ridge horn with DR-Lens tag in front. B: DR-Lens tag.

The results are produced by measurement of the S_{11} scattering parameter over 9-13 GHz using a double ridge horn (HF906 from R & S) with the DR-Lens tag placed on a Styrofoam ($\epsilon_r = 1.04$) block at about 60 cm in front of the horn aperture and positioned axially with the horn; pyramidal microwave absorbers were placed around the test range to avoid (time-variant) stray reflections from the lab environment. The low-level scattering from the DR-Lens tag is made visible by background subtraction, i.e., by first recording the scattering coefficient without the DR-Lens tag in place and consequently using the HP8510 Vector Network Analyzer subtraction operation on the measured data with the DR-Lens tag in place. The measured reflection coefficient of the DR-Lens tag is converted to RCS magnitudes by normalization to the reflection coefficient of a 20 mm dia. metal sphere at band centre and multiplication with its RCS; this method provides only approximate RCS magnitudes, since the frequency dependence of the horn antenna gain is not corrected for as in the method presented in [56]. The measurement setup is shown in Fig. 12.

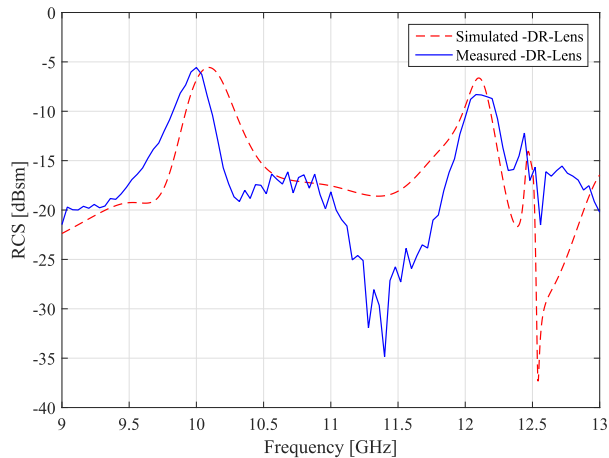


FIGURE 13. Measured RCS magnitudes compared to simulated RCS for DR-Lens tag.

Fig. 13 shows the measured RCS compared to the simulation results of Fig. 4. The results show a good agreement between measured and simulated monostatic scattering RCS at the tested frequency range. The same is predicted at THz frequencies by simply upscaling from 10.1 GHz to 105.6 GHz.

B. SIMULATION RESULTS

This section evaluates the proposed chipless RFID based localization system at THz band using the simulation scenario depicted in Fig. 1. An indoor area is considered, in which many reference DR-Lens tags are nested at the ceiling of the indoor environment assuming that each location within the environment is in the range of at least four tags in order to enable the objects inside the room localizing their self using Algorithm 1 with $N_{Ref} = 4$. Each DR-Lens tag is designed to have its unique frequency code as discussed in Section III-B. Assume an object is located in this area and also has a fixed-area antenna of $A_R = 100\text{ cm}^2$. The reader and the tags are designed to operate over the THz channel that is presented in Section III-C. LLS estimation method is used in order to determine the position after ranging step. The other simulation parameters are given in Table 1.

TABLE 1. DR-Lens based RFID localization system parameters.

Parameter	Value
Frequency Range	100 - 200 GHz
Operating Bandwidth	5 GHz
Transmit Power P_T	0 dBm
Noise Figure γ	20 dB
Room Width and Length	$10 \times 10\text{ m}^2$

To simplify the simulation process, the scanning phase is assumed to be performed using high SNR, in which the DR-Lens tags are detected and grouped perfectly. Moreover, for ranging purposes, a Gaussian pulse of 5 GHz bandwidth centered at the operating frequency f_n is used to interrogate

the the n^{th} tag with its resonance frequency f_n . For the sake of comparison, the location error is considered as

$$e = \sqrt{(\hat{x} - \bar{x})^2 + (\hat{y} - \bar{y})^2 + (\hat{z} - \bar{z})^2}. \tag{16}$$

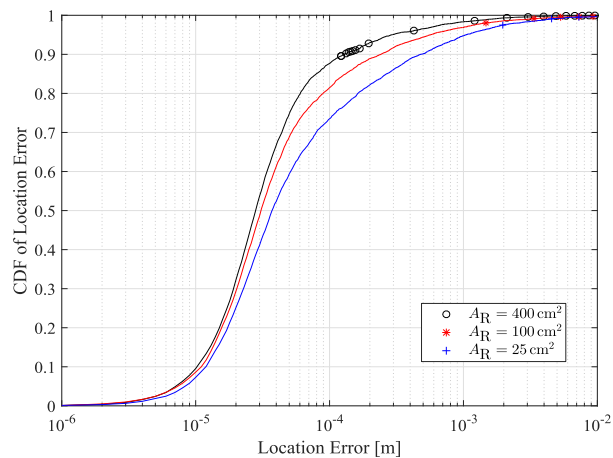


FIGURE 14. The CDF of location error for the proposed system for different A_R values.

Fig. 14 depicts the cumulative distribution function (CDF) of the location error for the proposed algorithm when the effective area of the reader antenna is $A_R = 400\text{ cm}^2$, $A_R = 100\text{ cm}^2$, and $A_R = 25\text{ cm}^2$. It is shown that the localization accuracy performance is getting better by increasing the gain of the reader antenna G_R . With the increase of A_R , the reader antenna gain G_R is increased, and hence the antenna directivity angle is decreased, which minimizes the multipath components and also interference area. When $A_R = 400\text{ cm}^2$, the location error is below 0.85 mm at 98% confidence. The location error is increased to 1.45 mm and 2.5 mm at 98% confidence when $A_R = 100\text{ cm}^2$ and $A_R = 25\text{ cm}^2$, respectively. We can say that millimeter-level accuracy becomes visible using the proposed system.

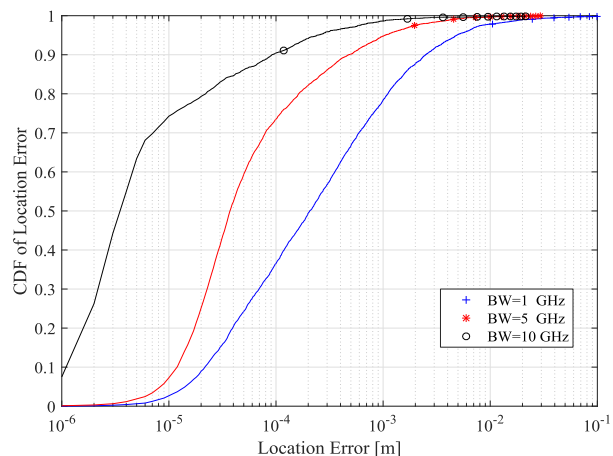


FIGURE 15. The CDF of location error for the proposed system for different pulse bandwidths.

Fig. 15 depicts the impact of the pulse bandwidth on localization accuracy when $A_R = 100\text{ cm}^2$. We note that the

localization accuracy is improved as the bandwidth of the pulse is increased due to reducing the possibility of overlapping between LoS and NLoS paths. The location error is less than 0.713 mm at 98% confidence when the pulse bandwidth equals 10 GHz. This error is increased to 1.45 mm and 1.1 cm at 98% confidence when the pulse bandwidth is decreased to 5 GHz and 1 GHz, respectively. The bandwidth is expected to have more effect when the reader antenna gain is decreased due to the existence of stronger NLoS paths and multi-tag interference.

VII. CONCLUSION AND OUTLOOK

In this work, we propose a THz based chipless RFID self-localization system using RToF based ranging in indoor environments. In the proposed system, the chipless tags act as the reference nodes that enables a smart object to self-localize. The tag side is designed as a combination between DR and lens in order to improve the RCS of the chipless tag and the coverage of the RFID link. Accordingly, the link budget of the proposed system is investigated, where the feasible spectral windows for RFID based localization are characterized. Moreover, we analyze the backscattered signal from a DR-Lens tag in order to perform ranging between this DR-Lens tag and the smart object using RToF. Afterwards, the reader position is determined using the relative distances between the reader and the reference tags using LLS approximation. Measurements are performed to examine the DR-Lens tag concept at low GHz-band, where close matching between the measured RCS and simulated one is obtained. This result opens the door for DR tag miniaturization towards sub-mm dimensions for achieving THz-functionality aiming at fabricating the DR-Lens tag at THz band in the near future. Numerical simulations are conducted at the THz-range to evaluate the overall localization system. The results show that the proposed system significantly improves the localization accuracy. 1.45 mm at 98% confidence of accuracy can be achieved when $A_R = 100 \text{ cm}^2$ and pulse bandwidth of 5 GHz. This level of accuracy even can be more improved by increasing the pulse bandwidth or the area of antenna at the reader side.

The proposed system is an efficient framework for the upcoming accurate localization systems. However, there are some implementation challenges that may affect the performance of the proposed system. One challenge is the DR-Lens tag response such as the angle-dependent and frequency-dependent response of the tag, which is a limitation for localization accuracy. Furthermore, RToF ranging depends on the pulse shape which could be affected by the hardware impairments such as antennas, reader, etc. These challenges will be investigated further in future research together with the practical implementation.

REFERENCES

- [1] H.-J. Song and T. Nagatsuma, "Present and future of terahertz communications," *IEEE Trans. THz Sci. Technol.*, vol. 1, no. 1, pp. 256–263, Sep. 2011.
- [2] A. Afsharinejad, A. Davy, B. Jennings, and C. Brennan, "Performance analysis of plant monitoring nanosensor networks at THz frequencies," *IEEE Internet Things J.*, vol. 3, no. 1, pp. 59–69, Feb. 2016.
- [3] H. Aggrawal, P. Chen, M. M. Assefzadeh, B. Jamali, and A. Babakhani, "Gone in a picosecond: Techniques for the generation and detection of picosecond pulses and their applications," *IEEE Microw. Mag.*, vol. 17, no. 12, pp. 24–38, Dec. 2016.
- [4] Y. Gu, A. Lo, and I. Niemegeers, "A survey of indoor positioning systems for wireless personal networks," *IEEE Commun. Surveys Tuts.*, vol. 11, no. 1, pp. 13–32, 1st Quart., 2009.
- [5] L. M. Ni, D. Zhang, and M. R. Souryal, "RFID-based localization and tracking technologies," *IEEE Wireless Commun.*, vol. 18, no. 2, pp. 45–51, Apr. 2011.
- [6] F. Zafari, A. Gkelias, and K. Leung. (2017). "A survey of indoor localization systems and technologies." [Online]. Available: <https://arxiv.org/abs/1709.01015>
- [7] K. Witrals, S. Hinteregger, J. Kulmer, E. Leitinger, and P. Meissner, "High-accuracy positioning for indoor applications: RFID, UWB, 5G, and beyond," in *Proc. IEEE Int. Conf. RFID*, May 2016, pp. 1–7.
- [8] Y. Ma, B. Wang, S. Pei, Y. Zhang, S. Zhang, and J. Yu, "An indoor localization method based on AOA and PDOA using virtual stations in multipath and NLOS environments for passive UHF RFID," *IEEE Access*, vol. 6, pp. 31772–31782, 2018.
- [9] K. Finkenzeller, *RFID Handbook: Fundamentals and Applications in Contactless Smart Cards and Identification*. Hoboken, NJ, USA: Wiley, 2003.
- [10] A. Costanzo et al., "Energy autonomous UWB localization," *IEEE J. Radio Freq. Identificat.*, vol. 1, no. 3, pp. 228–244, Sep. 2017.
- [11] F. Zheng and T. Kaiser, *Digital Signal Processing for RFID* (Information and Communication Technology Series). Hoboken, NJ, USA: Wiley, 2016.
- [12] S. Grebien et al., "Range estimation and performance limits for UHF-RFID backscatter channels," *IEEE J. Radio Freq. Identificat.*, vol. 1, no. 1, pp. 39–50, Mar. 2017.
- [13] N. Patwari, A. O. Hero, M. Perkins, N. S. Correal, and R. J. O'Dea, "Relative location estimation in wireless sensor networks," *IEEE Trans. Signal Process.*, vol. 51, no. 8, pp. 2137–2148, Aug. 2003.
- [14] S. Tomic, M. Beko, and R. Dinis, "3-D target localization in wireless sensor networks using RSS and AoA measurements," *IEEE Trans. Veh. Technol.*, vol. 66, no. 4, pp. 3197–3210, Apr. 2017.
- [15] N. Patwari, J. N. Ash, S. Kyperountas, A. O. Hero, R. L. Moses, and N. S. Correal, "Locating the nodes: Cooperative localization in wireless sensor networks," *IEEE Signal Process. Mag.*, vol. 22, no. 4, pp. 54–69, Jul. 2005.
- [16] M. Bolic, D. Simplot-Ryl, and I. Stojmenovic, *RFID Systems: Research Trends and Challenges*, 1st ed. Hoboken, NJ, USA: Wiley, 2010.
- [17] H. Liu, H. Darabi, P. Banerjee, and J. Liu, "Survey of wireless indoor positioning techniques and systems," *IEEE Trans. Syst., Man, Cybern. C, Appl. Rev.*, vol. 37, no. 6, pp. 1067–1080, Nov. 2007.
- [18] F. Guidi, A. Guerra, and D. Dardari, "Personal mobile radars with millimeter-wave massive arrays for indoor mapping," *IEEE Trans. Mobile Comput.*, vol. 15, no. 6, pp. 1471–1484, Jun. 2016.
- [19] F. Guidi, A. Sibille, C. Roblin, V. Casadei, and D. Dardari, "Analysis of UWB tag backscattering and its impact on the detection coverage," *IEEE Trans. Antennas Propag.*, vol. 62, no. 8, pp. 4292–4303, Aug. 2014.
- [20] R. E. Aneel and N. C. Karmakar, "Chipless RFID tag localization," *IEEE Trans. Microw. Theory Techn.*, vol. 61, no. 11, pp. 4008–4017, Nov. 2013.
- [21] M. Khaliel, A. El-Awamry, A. F. Megahed, and T. Kaiser, "A novel design approach for co/cross-polarizing chipless RFID tags of high coding capacity," *IEEE J. Radio Freq. Identificat.*, vol. 1, no. 2, pp. 135–143, Jun. 2017.
- [22] S. Priebe and T. Kürner, "Stochastic modeling of THz indoor radio channels," *IEEE Trans. Wireless Commun.*, vol. 12, no. 9, pp. 4445–4455, Sep. 2013.
- [23] C. Lin and G. Y. Li, "Indoor terahertz communications: How many antenna arrays are needed?" *IEEE Trans. Wireless Commun.*, vol. 14, no. 6, pp. 3097–3107, Jun. 2015.
- [24] D. Dardari, A. Conti, U. Ferner, A. Giorgetti, and M. Z. Win, "Ranging with ultrawide bandwidth signals in multipath environments," *Proc. IEEE*, vol. 97, no. 2, pp. 404–426, Feb. 2009.
- [25] Y. Shen and M. Z. Win, "Fundamental limits of wideband localization—Part I: A general framework," *IEEE Trans. Inf. Theory*, vol. 56, no. 10, pp. 4956–4980, Oct. 2010.
- [26] D. Dardari, R. D'Errico, C. Roblin, A. Sibille, and M. Z. Win, "Ultrawide bandwidth RFID: The next generation?" *Proc. IEEE*, vol. 98, no. 9, pp. 1570–1582, Sep. 2010.

- [27] S. Hinteregger, E. Leitinger, P. Meissner, and K. Witsral, "MIMO gain and bandwidth scaling for RFID positioning in dense multipath channels," in *Proc. IEEE Int. Conf. RFID*, May 2016, pp. 1–6.
- [28] N. Decarli, F. Guidi, and D. Dardari, "Passive UWB RFID for tag localization: Architectures and design," *IEEE Sensors J.*, vol. 16, no. 5, pp. 1385–1397, Mar. 2016.
- [29] D. Hotte, R. Siragusa, Y. Duroc, and S. Tedjini, "Radar cross-section measurement in millimetre-wave for passive millimetre-wave identification tags," *IET Microw., Antennas Propag.*, vol. 9, no. 15, pp. 1733–1739, 2015.
- [30] P. Pursula *et al.*, "Millimeter-wave identification—A new short-range radio system for low-power high data-rate applications," *IEEE Trans. Microw. Theory Techn.*, vol. 56, no. 10, pp. 2221–2228, Oct. 2008.
- [31] D. Wang, M. Fattouche, and X. Zhan, "Pursuance of mm-level accuracy: Ranging and positioning in mmWave systems," *IEEE Syst. J.*, to be published.
- [32] F. Guidi, N. Decarli, D. Dardari, F. Mani, and R. D'Errico, "Millimeter-wave beamsteering for passive RFID tag localization," *IEEE J. Radio Freq. Identificat.*, vol. 2, no. 1, pp. 9–14, Mar. 2018.
- [33] H. El-Sayed, G. Athanasios, and C. Fischione, "Evaluation of localization methods in millimeter-wave wireless systems," in *Proc. IEEE 19th Int. Workshop Comput. Aided Modeling Design Commun. Links Netw. (CAMAD)*, Dec. 2014, pp. 345–349.
- [34] N. Zhang, M. Hu, L. Shao, and J. Yang, "Localization of printed chipless RFID in 3-D space," *IEEE Microw. Wireless Compon. Lett.*, vol. 26, no. 5, pp. 373–375, May 2016.
- [35] T. Zhou *et al.*, "Short-range wireless localization based on meta-aperture assisted compressed sensing," *IEEE Trans. Microw. Theory Techn.*, vol. 65, no. 7, pp. 2516–2524, Jul. 2017.
- [36] M. El-Absi, A. Abuelhaija, A. Al-Haj Abbas, F. Zheng, K. Solbach, and T. Kaiser, "Chipless tags infrastructure based localization in indoor environments," in *Proc. German Microw. Conf. (GeMiC)*, Mar. 2018, pp. 267–270.
- [37] M. Werner, *Indoor Location-Based Services: Prerequisites and Foundations*. Cham, Switzerland: Springer, 2014.
- [38] B. Kubina, M. Schübler, C. Mandel, A. Mehmood, and R. Jakoby, "Wireless high-temperature sensing with a chipless tag based on a dielectric resonator antenna," in *Proc. IEEE SENSORS*, Nov. 2013, pp. 1–4.
- [39] C. Mandel, B. Kubina, M. Schübler, and R. Jakoby, "Metamaterial-inspired passive chipless radio-frequency identification and wireless sensing," *Ann. Telecommun.*, vol. 68, nos. 7–8, pp. 385–399, Aug. 2013, doi: 10.1007/s12243-013-0372-9.
- [40] A. A. Abbas, M. El-Absi, A. A. K. Solbach, and T. Kaiser, "Passive chipless tag based on dielectric resonator-lens combination," to be published.
- [41] R. K. Mongia and P. Bhartia, "Dielectric resonator antennas—A review and general design relations for resonant frequency and bandwidth," *Int. J. Microw. Millim.-Wave Comput.-Aided Eng.*, vol. 4, no. 3, pp. 230–247, 1994.
- [42] A. Ramos, E. Perret, O. Rance, S. Tedjini, A. Lázaro, and D. Girbau, "Temporal separation detection for chipless depolarizing frequency-coded RFID," *IEEE Trans. Microw. Theory Techn.*, vol. 64, no. 7, pp. 2326–2337, Jul. 2016.
- [43] B. S. Çiftler, A. Kadri, and I. Güvenç, "IoT localization for bistatic passive UHF RFID systems with 3-D radiation pattern," *IEEE Internet Things J.*, vol. 4, no. 4, pp. 905–916, Aug. 2017.
- [44] T. Schneider, A. Wiatrek, S. Preußler, M. Grigat, and R.-P. Braun, "Link budget analysis for terahertz fixed wireless links," *IEEE Trans. THz Sci. Technol.*, vol. 2, no. 2, pp. 250–256, Mar. 2012.
- [45] P. Boronin, D. Moltchanov, and Y. Koucheryavy, "A molecular noise model for THz channels," in *Proc. IEEE Int. Conf. Commun. (ICC)*, Jun. 2015, pp. 1286–1291.
- [46] N. J. Kinzie, "Ultra-wideband pulse Doppler radar for short-range targets," Ph.D. dissertation, Elect., Comput. Energy Eng., Univ. Colorado Boulder, Boulder, CO, USA, 2011.
- [47] J. P. Stralka and W. G. Fedarko, *Radar Handbook: Pulse Doppler Radar*, 3rd ed. New York, NY, USA: McGraw-Hill, 2008, ch. 4.
- [48] R. Measel, C. S. Lester, Y. Xu, R. Primerano, and M. Kam, "Detection performance of spread spectrum signatures for passive, chipless RFID," in *Proc. IEEE Int. Conf. RFID*, Apr. 2014, pp. 55–59.
- [49] A. El-Awamry, M. Khaliel, A. Fawky, and T. Kaiser, "A novel multi-tag identification technique for frequency coded chipless RFID systems based on look-up-table approach," in *Proc. 11th Eur. Conf. Antennas Propag. (EUCAP)*, Mar. 2017, pp. 2070–2074.
- [50] F. J. Álvarez, T. Aguilera, J. A. Paredes, and J. A. Moreno, "Acoustic tag identification based on noncoherent FSK detection with portable devices," *IEEE Trans. Instrum. Meas.*, vol. 67, no. 2, pp. 270–278, Feb. 2018.
- [51] P. Kalansuriya, N. C. Karmakar, and E. Viterbo, "On the detection of frequency-spectra-based chipless RFID using UWB impulsive interrogation," *IEEE Trans. Microw. Theory Techn.*, vol. 60, no. 12, pp. 4187–4197, Dec. 2012.
- [52] A. A.-H. Abbas, A. Abuelhaija, and K. Solbach, "Investigation of the transient EM scattering of a dielectric resonator," in *Proc. 11th German Microw. Conf. (GeMiC)*, Mar. 2018, pp. 271–274.
- [53] C. Gentile, N. Alsindi, R. Raulefs, and C. Teolis, *Geolocation Techniques: Principles and Applications*. New York, NY, USA: Springer, 2012.
- [54] R. L. Haupt, *Antenna Arrays: A Computational Approach*. Hoboken, NJ, USA: Wiley, 2010.
- [55] V. Petrov, M. Komarov, D. Moltchanov, J. M. Jornet, and Y. Koucheryavy, "Interference and SINR in millimeter wave and terahertz communication systems with blocking and directional antennas," *IEEE Trans. Wireless Commun.*, vol. 16, no. 3, pp. 1791–1808, Mar. 2017.
- [56] P. V. Nikitin and K. V. S. Rao, "Theory and measurement of backscattering from RFID tags," *IEEE Antennas Propag. Mag.*, vol. 48, no. 6, pp. 212–218, Dec. 2006.



MOHAMMED EL-ABSI received the B.E. degree from the Islamic University of Gaza, Gaza, Palestine, in 2005, the M.S. degree from the Jordan University of Science and Technology in 2008, and the Ph.D. degree (*summa cum laude*) from the University of Duisburg-Essen, Duisburg, Germany, in 2015, all in electrical engineering. He is currently a Mercator Fellow with the Collaborative Research Center's Mobile Material Characterization and Localization by Electromagnetic Sensing Project at the Digital Signal Processing Institute, University of Duisburg-Essen. His research interests are in the area of communication and signal processing. He received the German Academic Exchange Service Fellowship in 2006 and 2011.



ALI ALHAJ ABBAS received the B.Sc. degree in electrical/communication engineering from Yarmouk University, Irbid, Jordan, in 2010, and the M.Sc. degree from the University of Jordan, Amman, Jordan, in 2016. He is currently pursuing the Ph.D. degree with the Institute of Digital Signal Processing, University of Duisburg-Essen. From 2011 to 2017, he was a Teaching Assistant and a Lecturer with Applied Science Private University, Jordan. He is currently a Research Fellow with the Collaborative Research Center for the Project Mobile Material Characterization and Localization by Electromagnetic Sensing, University of Duisburg-Essen. His current research interests are in the area of antennas and RF technologies, UWB antennas, and chipless RFID tags.



ASHRAF ABUELHAJJA received the B.Sc. degree in communications and electronics engineering from Applied Science Private University, Amman, Jordan, in 2007, and the master's and Ph.D. degrees in electrical engineering from the University of Duisburg-Essen in 2010 and 2016, respectively. From 2012 to 2014, he was a Research Assistant with the Erwin L. Hahn Institute for Magnetic Resonance Imaging, Essen. From 2014 to 2016, he was a Research Assistant

with the Department of Microwave and RF Technology, University of Duisburg-Essen. He is currently an Assistant Professor with the Department of Electrical Engineering, Applied Science Private University. His research interests are in the area of antennas and RF technology.



FENG ZHENG received the B.Sc. and M.Sc. degrees in electrical engineering from Xidian University, Xi'an, China, in 1984 and 1987, respectively, and the Ph.D. degree in automatic control from the Beijing University of Aeronautics and Astronautics, Beijing, China, in 1993. Previously, he held the Alexander-von-Humboldt Research Fellowship with the Gerhard Mercator University of Duisburg, Germany, and research positions at Tsinghua University, Beijing, the National University of Singapore, Singapore, and the University of Limerick, Ireland.

From 1995 to 1998, he was with the Center for Space Science and Applied Research, Chinese Academy of Sciences, Beijing, as an Associate Professor. From 2007 to 2011, he was with the Institute of Communications Technology, Leibniz University of Hannover, Hannover, Germany, as the Leader of the Research Group Applied Signal Processing. Since 2011, he has been with the Institute of Digital Signal Processing, Faculty of Engineering, University of Duisburg-Essen, Duisburg, Germany, as the Leader of the Research Group Algorithm Design and Analysis. His research interests include RFID, UWB-MIMO, wireless communications, signal processing, and systems and control theory. In these areas, he published two books *Ultra Wideband Systems with MIMO* (Wiley, 2010), *Digital Signal Processing for RFID* (Wiley, 2016), and a number of journal/conference papers. He was a co-recipient of several awards, including the Best Paper Award in 1994 from the Society of Instrument and Control Engineering of Japan at the 33rd SICE Annual Conference, Tokyo, Japan, the Science and Technology Achievement Award (first Award) in 1997 from the State Education Commission of China, and the National Natural Science Award (third Award) in 1999 from the Chinese Government.



KLAUS SOLBACH was with the University of Duisburg-Essen as a Junior Researcher in the field of integrated dielectric image line circuits from 1975 to 1980. In 1981, he joined the Millimeterwave Research Laboratory, AEG-Telefunken, Ulm, and in 1984, he moved to the Radar Systems Group, Daimler-Benz Aerospace (currently a part of Airbus Group), where he involved in the design and production of microwave-subsystems for ground-based and airborne Radar, EW, and

communication systems, including phased array and active phased array antenna systems. His last position was the Manager of the RF-and-Antenna-Subsystems Department. In 1997, he joined the Faculty of the University of Duisburg-Essen as the Chair of RF and microwave technology. He has authored and co-authored over 200 national and international papers, conference contributions, book chapters, and patent applications. He was the Chairman of the VDE-ITG Fachausschuss Antennen, an Executive Secretary of the Institut für Mikrowellen-und Antennentechnik, and the Chair of the IEEE Germany AP/MTT Joint Chapter. He was a General Chair of the International ITG-Conference on Antennas INICA2007, Munich, and the European Conference on Antennas and Propagation EuCAP2009, Berlin.



THOMAS KAISER (M'98–SM'04) received the Diploma degree in electrical engineering from Ruhr-University Bochum, Bochum, Germany, in 1991, and the Ph.D. (Hons.) and German Habilitation degrees in electrical engineering from Gerhard Mercator University, Duisburg, Germany, in 1995 and 2000, respectively. From 1995 to 1996, he spent a research leave with the University of Southern California, Los Angeles, which was grant-aided by the German Academic

Exchange Service. From 2000 to 2001, he was the Head of the Department of Communication Systems, Gerhard Mercator University, and from 2001 to 2002, he was the Head of the Department of Wireless Chips and Systems, Fraunhofer Institute of Microelectronic Circuits and Systems, Duisburg. From 2002 to 2006, he was a Co-Leader of the Smart Antenna Research Team, University of Duisburg-Essen, Duisburg. In summer of 2005, he joined the Smart Antenna Research Group, Stanford University, Stanford, CA, USA, as a Visiting Professor, and in winter of 2007, he joined the Department of Electrical Engineering, Princeton University, Princeton, NJ, USA, as a Visiting Professor. From 2006 to 2011, he headed the Institute of Communication Technology, Leibniz University of Hannover, Germany. He is currently the Head of the Institute of Digital Signal Processing, University of Duisburg-Essen, and is also the Founder and the CEO of ID4us GmbH, an RFID centric company. He has authored and co-authored over 300 papers in international journals and conference proceedings and two books *Ultra Wideband Systems with MIMO* (Wiley, 2010) and *Digital Signal Processing for RFID* (Wiley, 2015). He is the Speaker of the Collaborative Research Center Mobile Material Characterization and Localization by Electromagnetic Sensing. He was the Founding Editor-in-Chief of the e-letter of the IEEE Signal Processing Society and a General Chair of the IEEE International Conference on UltraWideBand in 2008, the International Conference on Cognitive Radio Oriented Wireless Networks and Communications in 2009, the IEEE Workshop on Cellular Cognitive Systems in 2014, and the IEEE Workshop on Mobile THz Systems in 2018.

• • •